

NeuroDeX: Unlocking Diverse Support in Decompiling Deep Neural Network Executables

Yilin Li

Institute of Information Engineering,

CAS

School of Cybersecurity, UCAS

Beijing, China

liyilin2023@iie.ac.cn

Guozhu Meng*

Institute of Information Engineering,

CAS

School of Cybersecurity, UCAS

Beijing, China

mengguozhu@iie.ac.cn

Mingyang Sun

Institute of Information Engineering,

CAS

School of Cybersecurity, UCAS

Beijing, China

sunmingyang@iie.ac.cn

Yanzhong Wang

Institute of Information Engineering,

CAS

School of Cybersecurity, UCAS

Beijing, China

wangyanzhong@iie.ac.cn

Kun Sun

Institute of Information Engineering,

CAS

School of Cybersecurity, UCAS

Beijing, China

sunkun2023@iie.ac.cn

Hailong Chang

Institute of Information Engineering,

CAS

School of Cybersecurity, UCAS

Beijing, China

changhailong@iie.ac.cn

Yuekang Li

University of New South Wales

Sydney, Australia

yuekang.li@unsw.edu.au

Abstract—On-device deep learning models have extensive real-world demands. Deep learning compilers efficiently compile models into executables for deployment on edge devices, but these executables may face the threat of reverse engineering. Previous studies have attempted to decompile DNN executables, but they face challenges in handling compilation optimizations and analyzing quantized compiled models.

In this paper, we present NeuroDeX to unlock diverse support in decompiling DNN executables. NeuroDeX leverages the semantic understanding capabilities of LLMs along with dynamic analysis to accurately and efficiently perform operator type recognition, operator attribute recovery and model reconstruction. NeuroDeX can recover DNN executables into high-level models towards compilation optimizations, different architectures and quantized compiled models. We conduct experiments on 96 DNN executables across 12 common DNN models. Extensive experimental results demonstrate that NeuroDeX can decompile non-quantized executables into nearly identical high-level models. NeuroDeX can recover functionally similar high-level models for quantized executables, achieving an average top-1 accuracy of 72%. NeuroDeX offers a more comprehensive and effective solution compared to previous DNN executables decompilers.

I. INTRODUCTION

In recent years, deep learning (DL) has rapidly advanced in the real world. Deploying deep neural networks (DNNs) on edge devices can meet the real-time requirements of edge computing, enhance privacy protection and enable offline inference capabilities, making DNNs widely applicable in real-world scenarios [2], [6], [21], [45]. DL compilers, such as TVM [3] and GLOW [37], can compile high-level DNN

models into executables for inference on edge devices. DNNs are composed of different operators (e.g., *Conv*, *Relu*), and DL compilers compiles these operators into operator functions in executables. DL compilers optimize models during compilation to improve inference efficiency, which provides a good solution for deploying models on edge devices [22], [25], [55].

In DNN executables, the operators and weights are compiled into incomprehensible machine code, thereby reducing the risk of model extraction attacks compared to white-box deployment. However, DNN executables may still pose security risks due to decompilation. DNN executables can potentially be decompiled to original high-level models. This undermines the intellectual property of the model owners, especially for models trained on private data. Based on the recovered high-level models, attackers can perform white-box adversarial attacks and backdoor attacks, threatening the secure use of DNN executables.

Previous works [27], [42], [53], [54], [59] have attempted to decompile DNN binaries, but the existing methods have certain limitations. They struggle to simultaneously address compilation optimizations, support different architectures, and accommodate quantized compiled model, all of which are essential for meeting the demands of modern DL applications. These limitations can be summarized as follows. **L1**: The recognition for operator types is not accurate enough, previous methods struggle to handle fused operators under compilation optimization and rely on prior knowledge such as compiler versions. **L2**: The current cross-architecture decompilers rely on relatively heavy analysis methods or support too few

*Corresponding author.

types of operators. They also cannot analyze fused operators. **L3:** Previous works lack consideration for quantized models, which is a common inference optimization strategy for edge devices.

To address these limitations, we propose NeuroDeX to unlock diverse support in decompiling DNN executables. NeuroDeX begins by collecting operator function information including disassembled and decompiled code from DNN executables. Next, NeuroDeX utilizes the semantic understanding abilities of LLMs to design an accurate and scalable method for operator type recognition. Subsequently, NeuroDeX utilizes dynamic analysis and LLM-based code understanding to finish operator attribute recovery. Finally, NeuroDeX reconstructs the model’s computational graph and weights through dynamic analysis. NeuroDeX features an accurate operator type recognition and operator attribute recovery mechanism that does not rely on prior knowledge such as compiler versions or training data. NeuroDeX can accurately recover fused operators and its core components do not depend on resource-intensive analysis techniques like symbolic execution, allowing for rapid and efficient analysis. Furthermore, NeuroDeX is extendable to different architectures, different DL compilers, and quantized models.

NeuroDeX is evaluated on 88 non-quantized DNN executables and NeuroDeX can accurately recover them into nearly identical high-level models. NeuroDeX adapts for the different compiler versions, accommodates a wider range of models, and supports different architectures. The operator type recognition accuracy for all TVM executables and GLOW executables reaches 99.22% and 97.62% respectively. The operator attribute recovery accuracy is nearly 100%. NeuroDeX incorporates robust error fix strategies, and **all** the recovered model’s inference accuracy reaches 100% after the errors are fixed. Additionally, we evaluate NeuroDeX on 8 quantized compiled DNN executables, the results indicate that NeuroDeX can successfully recover functionally similar high-level models. For model inference, the average top_1 accuracy is 72%, and the average top_5 accuracy is 86%.

Our contributions are summarized as follows:

- We propose NeuroDeX to provide diverse support in decompiling DNN executables. It can decompile DNN executables into high-level models towards different DL compilers, different architectures and quantized compiled models.
- We design a mechanism that leverages the semantic understanding capabilities of LLMs along with dynamic analysis to accurately and efficiently perform operator type recognition and operator attribute recovery, overcoming the limitations of previous works.
- We conduct experiments on 96 DNN executables across 12 common DNN models. Extensive experimental results demonstrate that NeuroDeX can successfully decompile various types of DNN executables, providing more comprehensive support than previous decompilers.

II. FOUNDATION AND PROBLEM STATEMENT

A. Deep Learning Compiler

DNNs are computational models consisting of multiple layers. These layers are constructed from different types of operators that perform various mathematical computations (e.g., *Conv*, *Relu*), and some operators have attributes (e.g., stride in *Conv*). Subsequent operators take the outputs of previous operators as their inputs, and the connection topology of these different operators constructs the model’s computational graph. The inputs and outputs of operators are four-dimensional tensors in $[batch_num, channel, height, width]$ format. During model inference, data is propagated through the computational graph until the final output is obtained. Quantization is a technique that reduces the precision of model weights. This process significantly decreases memory and computational requirements, enabling efficient inference on resource-limited edge devices, typically with minimal loss in accuracy.

DL compilers provide valuable solutions for deploying DNNs on edge devices. DL compilers perform a series of optimizations on these operators and ultimately compile them into executables. The operators are compiled into functions in executables, the inputs and outputs of a operator correspond in sequence to the parameters of the operator function. The compiled executables can efficiently perform inference on resource-constrained edge devices. DL compilers also support quantized compiled models, which further reduces the resource consumption of model inference.

The general workflow of a DL compiler involves three steps: *frontend processing*, which converts general model representations, such as ONNX [33], into computational graphs supported by the compiler’s frontend; *compilation optimization*, applying various optimization techniques, including high-level optimizations like operator fusion and constant folding, and low-level optimizations such as layout rearrangement; *code generation*, which generates executables adapted for the target device’s hardware.

B. DNN Executables Decompiler

The goal of DNN decompiler is to reverse DNN executables into identical high-level models. The typical workflow of DNN executables decompiler involves the three steps: *operator type recognition*, determining the specific type of DNN operator functions; *operator attribute recovery*, which recovers attribute values for operators, such as the stride for *Conv*; *model reconstruction*, rebuilding the computational graph and collecting operator weights to reconstruct high-level models within a general DL framework like PyTorch [34].

C. Research Gap

DNN executables are typically deployed offline on edge devices, and attackers can reverse them to high-level DNN models, which can damage the intellectual property of the model owners, especially for models trained on private data [32]. Moreover, based on the recovered high-level models, attackers can employ methods such as white-box adversarial

TABLE I: Comparison with Existing DNN Decompilers

Works	Optim	Cross Arch	Quant
Libsteal [59]	○	○	○
Shi et al [42]	○	○	○
DND [53]	○	●	○
Neuroscope [54]	○	●	○
BTD [27]	●	○	○
NeuroDeX	●	●	●

attacks [10], [26], [31] and backdoor attacks [23], [38] on the DNN executables. These potential attacks can be directly implemented by editing executables and are difficult to detect, further increasing security risks.

Previous works [27], [42], [53], [54], [59] have attempted to decompile DNN binaries. However, each of these methods has its limitations. We summarize the previous works and compare them with NeuroDeX in Table I. Libsteal cannot decompile standalone DNN executables and is unable to handle compilation optimizations. The accuracy of the models recovered by Libsteal is relatively low. The work by Shi et al. only supports x86 architecture and cannot recover models with high accuracy. DND and Neuroscope do not effectively handle compilation optimizations. DND relies on symbolic execution methods, which incur significant overhead and limit the size of supported models; Neuroscope only supports 12 DNN operators. Although BTD considers the impact of compilation optimizations, its operator type recognition method relies on prior knowledge like compiler versions, presenting challenges for extensibility, and it only supports x86 architecture. Moreover, all previous works overlook models compiled with quantization, which limits the applicability of these methods in practical scenarios.

Previous DNN executables decompilers have their own limitations and existing decompilers struggle to simultaneously address compilation optimizations, support different architectures, and accommodate quantized compiled models. We summarize the challenges faced as follows. **C1:** A method for accurate operator type recognition needs to be designed. It should be able to cover a wide variety of operators and fused operators under compilation optimization. The method should not rely on prior knowledge such as compiler version or training data. **C2:** A decompiler needs to integrate the new method for operator type recognition, forming an end-to-end pipeline that recover DNN executables into high-level models. The decompiler should also have cross-architecture support capabilities. **C3:** Quantized compiled models exhibit new characteristics different from standard models, involving quantization scaling factors between integer and float domains. The decompiler needs to be compatible with these differences.

To address these challenges, we design NeuroDeX to implement a more comprehensive decompiler for DNN executables.

For C1: We systematically analyze the characteristics of operators in DL compilers and design a progressive operator type recognition strategy. NeuroDeX leverages dynamic analysis and code semantic understanding from LLMs to support com-

patibility with various types of operators and fused operators. **For C2:** Based on the operator type recognition method, we subsequently implement operator attribute recovery and model reconstruction, forming a complete decompilation pipeline compatibility with various types of different models. The core technology of NeuroDeX is hardware-platform independent, ensuring its cross-architecture support capabilities. **For C3:** NeuroDeX specifically adapts the model reconstruction method to convert integer domain weights back to float domain. NeuroDeX employs a learning-based weights recovery approach that requires only a small amount of training data to recover functionally very similar models.

D. Threat Model

NeuroDeX is designed towards DNN executables deployed on edge devices, where NeuroDeX can access DNN executables compiled by DL compilers and extract the complete executables. DNN executables are generated through standard DL compiler pipeline with optional compiler optimization. NeuroDeX has the capability to execute the executables and monitor memory status during execution. NeuroDeX requires no prior knowledge of model architecture or weights, it only needs trivial inputs that satisfy the expected input format. The ultimate goal of NeuroDeX is to decompile executables into identical white-box high-level DL models, effectively extracting the computational graph, weights and other information.

The threat model used in our study is consistent with previous works [27], [42], [53], [54] and is generally common and practical in real-world scenarios. The design of NeuroDeX aims to highlight security risks of DNN executables and promote the safe use of DL compilers.

III. APPROACH

As shown in Figure 1, NeuroDeX is designed as an universal pipeline for different types of DNN executables, enabling end-to-end recovery of DNN executables into high-level models. Specifically, NeuroDeX first extracts operator function information, such as disassembled code, decompiled code and parameter dimensions from DNN executables. In this stage, NeuroDeX utilizes Ghidra [9], a general-purpose decompiler. Secondly, NeuroDeX completes operator type recognition and operator attribute recovery, where it leverages dynamic analysis and code semantic understanding from LLMs to support compatibility with various types of models. Dynamic analysis aims to monitor the runtime information of operator functions, and LLMs can understand the mathematical semantics of operators in decompiled code without relying on prior knowledge like compiler versions or training data. Finally, NeuroDeX performs model reconstruction by computational graph and model weights recovery, recovering high-level models. Next, we will sequentially introduce the components of NeuroDeX.

A. Operator Function Extraction

NeuroDeX first collects operator function information including disassembled and decompiled code from DNN executables using ghidra.

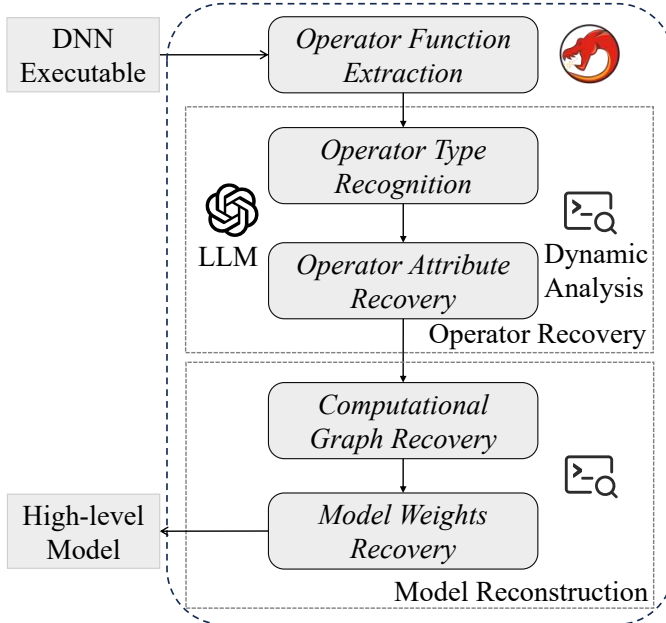


Fig. 1: Workflow of NeuroDeX

Inspired by previous works [42], [59], NeuroDeX can identify the dimensions of operator parameters from disassembled code in TVM compiler. NeuroDeX further expands on their methods, NeuroDeX also extracts the types of operator parameters and recover the optimized parameters' dimensions. The parameters' types can help determine the weights of quantized compiled models. The recovery of optimized parameters' dimensions can help analyze optimized operators. Figure 2 is a specific example of *Transform* operator. The parameters' dimensions and types can be extracted by scanning the disassembled code.

The dimension of the first parameter is optimized into $[N, C, H, W, c]$ layout. NCHWc [3] is a commonly used inference optimization method, which adapts to hardware and accelerates inference. NeuroDeX can recover it into standard $[N, C * c, H, W]$ format. Similarly, the dimension $[O_c, I_c, K, K]$ of a *Conv* kernel parameter may be optimized into $[O_c/A, I_c/B, K, K, B, A]$ [3]. The optimized layout decides the storage order of model weights in memory. NeuroDeX extracts this optimized dimension layout and converts it to standard format. The parameters of the function correspond sequentially to the inputs and outputs of the operator. Each type operator has a fixed number of inputs and outputs, and NeuroDeX can accurately recover parameters' dimensions. We validate this characteristic across both historical and recent TVM versions, ensuring the generality and robustness of our approach.

B. Operator Type Recognition

The purpose of operator type recognition is to determine the specific type of the operator function. Prior studies have limitations in operator type recognition. For instance, BTD relies

```

cmp edx, 0x2; jnz 0x402fa0;
=>param num is: 2
...
cmp [rdx + 0x16], 0x1; jnz 0x403025;
cmp [rdx + 0x15], 0x20; jnz 0x403025;
cmp [rdx + 0x14], 0x2; jnz 0x403025;
=>param1's type is: float32
cmp [rcx], 0x1; jnz 0x403038;
cmp [rcx + 0x8], 0x1c; jnz 0x40304b;
cmp [rcx + 0x10], 0x1c; jnz 0x40305e;
cmp [rcx + 0x18], 0x1c; jnz 0x403071;
cmp [rcx + 0x20], 0x4; jnz 0x403084;
=>param1's dimension is: [1,28,28,28,4]
...
cmp [rax + 0x16], 0x1; jnz 0x4030e3;
cmp [rax + 0x15], 0x20; jnz 0x4030e3;
cmp [rax + 0x14], 0x2; jnz 0x4030e3;
=>param2's type is: float32
cmp [r10], 0x1; jnz 0x4030f6;
cmp [r10 + 0x8], 0x70; jnz 0x403109;
cmp [r10 + 0x10], 0x1c; jnz 0x40311c;
cmp [r10 + 0x18], 0x1c; jnz 0x40312f;
=>param2's dimension is: [1,112,28,28]

```

Fig. 2: An Example of Disassembled Code

on training on specific data of each compiler version, DND and Neuroscope perform bad in handling fused operators.

We manually analyze DL compiler's support for DNN operators, and the operators can be divided into four types as shown in Table II. Type 1 is *Layout Transformation*. This type of operator adjusts the layout of input tensors and it can be further divided into inter-tensor types like *Concat* and intra-tensor types like *Flatten*. Inter-tensor types involve layout adjustments across multiple tensors, whereas intra-tensor refers to layout adjustments only to a single input tensor. Type 2 is *Element-wise*. This type of operator performs element-wise computation on the input tensor. It can be further divided into type 2.1 with two operands (one input and one output) like *Softmax* and type 2.2 with three operands (two inputs and one output) like *Add*. Type 3 is *Reduction*. This type of operator performs feature reduction on the input tensor, such as *Maxpool*. The output tensor is usually compressed in size compared to the input tensor. Type 4 is *Complex*. This type of operator performs complex and intensive computations, such as *Conv*. Due to the optimization of DL compilers, multiple operators may be fused into one operator to accelerate inference. TVM refers to enabling no optimization as “O0”, while enabling full optimizations as “O3”. GLOW applies full optimizations by default. Next, we will introduce the specific methods of operator type recognition towards TVM

TABLE II: Operator Classification

Type	Operators	Description
1. Layout Transformation	1.1 concat, split... 1.2 flatten, reshape, transpose...	Inter-tensor layout transformation Intra-tensor layout transformation
2. Element-wise	2.1 softmax, sqrt, clip, abs, relu... 2.2 add, sub, mul, div, power...	Element-wise computation of two operands Element-wise computation of three operands
3. Reduction	3.1 maxpool, avgpool, sum, max...	Feature reduction and extraction
4. Complex	4.1 conv, dense...	Complex and intensive computation

and GLOW.

For TVM, as parameters' dimensions of operator function can be collected during the operator function extraction phase, NeuroDeX uses them to enhance operator type recognition. Operators can undergo coarse-grained identification of their types. For *Layout Transformation* type and *Complex* type, specific operator types can be directly determined. For example, an operator with two parameters' dimensions: [1, 1000, 1, 1] and [1, 1000] can be directly identified as *Flatten*. For *Conv*, input channel and output channel of kernel parameter correspond respectively to the channel of the first and last parameters. For *Element-wise* and *Reduction* type, operators can be determined candidate list among 2.1, 2.2, 3.1 in Table II according to the number and dimension of parameters. Further, leveraging the code semantic understanding capabilities of LLMs, NeuroDeX determines the specific operator types within the candidate list based on the mathematical features of the decompiled code. This approach overcomes the limitations of previous methods, which rely heavily on training data and struggle with the cross-version support for compilers. Here is the simplified prompt for specific operator type recognition:

Simplified prompt of operator type recognition

You are an AI assistant specialized in analyzing operators. Given the decompiled code of an operator: {pseudocode}, identify the operator as one of {candidates}.

At the O3 optimization level, operators frequently undergo fusion. The most common operator fusion occurs *Conv* and *Dense* with the operators following them. NeuroDeX identifies their types through dynamic analysis. As shown in Algorithm 1, for *Conv* and *Dense*, during operator fusion, they are fused with several *Multiply* or *Add* operators, which are typically related to bias addition, batch normalization, etc. Specifically, NeuroDeX records the parameter addresses of each operator function through dynamic instrumentation. If the input is the output of previous operators, this indicates a skip connection (jumpadd). Otherwise, NeuroDeX starts recording the memory access during the operator function execution, identifying the instruction that initially accesses the parameter address. From this instruction, NeuroDeX performs taint analysis, tracking relevant registers until first encounter a multiply or add instruction. Activation functions like *Relu*

Algorithm 1: Fused Operator Type Recognition

```

Input: Operator:  $op(conv/dense)$ 
Output: Operator_type:  $fuse\_type$ 
 $fuse\_type \leftarrow op.base\_type;$ 
 $param\_addrs \leftarrow \log\_param\_addrs(op);$   $\triangleright$  record
    function parameter addresses
for  $i = 2$  to  $param\_addrs.length - 1$  do
    if  $param\_addrs[i] \in prev\_ops.output$  then
         $fuse\_type \leftarrow fuse\_type + "jumpadd";$ 
    else
         $start \leftarrow \text{mem\_read\_first}(op, param\_addrs[i]);$ 
         $\triangleright$  record the instruction address
        that first reads the param
         $fuse\_type \leftarrow fuse\_type + \text{taint}(op, start);$ 
         $\triangleright$  taint propagation until
        determine mul or add
     $fuse\_type \leftarrow fuse\_type + \text{check\_activation}(op);$ 
     $\triangleright$  check activation and
    activation_type
return  $fuse\_type$ 

```

and *Clip* are often attached to the tail of the fused operator with repeated patterns in decompiled code. NeuroDeX extracts the tail part of the decompiled code and uses LLM to verify if activation is accompanied by the fused operator. Similarly, for the fused operator consisting of *Concat* and activation, NeuroDeX employs the same processing method. NeuroDeX provides more comprehensive analysis and support for fused operators than previous works.

For GLOW, the disassembled code does not contain dimension information, but the optimization strategy in GLOW is relatively simple. Operator fusion almost only occurs after *Conv* with activation. NeuroDeX directly performs operator type recognition by classifying the decompiled code with LLM, which considers all operators as the candidate list and determines the specific operator types within the candidate list based on the mathematical features of operators.

Currently, NeuroDeX supports the most common operators of ONNX, the complete list of operators can be found in Appendix IX-A. We compile and decompile validated computer vision models from the ONNX Model Zoo, and NeuroDeX can cover all the operators of them. The operator type recognition method of NeuroDeX has good scalability. For more operators,

it only requires defining their types in Table II. The pipeline of operator type recognition in NeuroDeX is universal and scalable.

C. Operator Attribute Recovery

Some operators contain specific attribute value, such as the stride and padding of *Conv*. To ensure the functional consistency of the reconstructed model, it is essential to accurately recover these attributes. NeuroDeX combines dynamic analysis and code semantic understanding from LLM to design attribute recovery methods for different operators.

For *Conv*, NeuroDeX utilizes parameters' dimensions of these operators to recover attributes. For TVM, dimensions have been collected from disassembled code introduced in operator function extraction. For GLOW, NeuroDeX employs dynamic analysis to collect parameters' dimensions. The *Conv* in GLOW has four parameters: *out*, *in*, *weight* and *bias*. NeuroDeX records the memory read ranges starting from these four parameters. NeuroDeX first extracts *kernel_size* from decompiled code, the *kernel_size* is manifested as two continuous outer loop with identical values in decompiled code (An example can be found in Appendix IX-B). The output channel is equal to the number of weights read from the *bias* parameter. Next, the following relationships can be used:

$$\text{in_channel} = \frac{\text{weight_region}}{\text{out_channel} \times \text{kernel_size}^2} \quad (1)$$

For *Maxpool* and *Avgpool*, NeuroDeX extracts channel value from decompiled code, which corresponds to the inner loops following two identical loops (An example can be found in Appendix IX-B). NeuroDeX records the ranges of input and output. Next, the following relationships can be used:

$$\text{in_height/out_height} = \sqrt{\frac{\text{region}}{\text{channel}}} \quad (2)$$

Algorithm 2 explains how NeuroDeX accomplishes operator attribute recovery. For *Conv* or *Pooling* operators, the *input_height*, *output_height* and *kernel_size* are inherently contained within the parameters' dimensions. The *input_height* I_h , *padding* P , *kernel_size* K , *stride* S , and *output_height* O_h satisfy the following constraint:

$$O_h = \left\lceil \frac{(I_h + 2P - K)}{S} \right\rceil + 1 \quad (3)$$

Except for stride and padding, all other variables for *Conv* are known, and both stride and padding must be integers. To determine the values of them, NeuroDeX employs a constraint enumeration method. Starting with stride = 1 and padding = 0, NeuroDeX enumerates different combinations in ascending order to find solution that satisfies the constraint.

For *Avgpool* and *Maxpool*, *kernel_size* does not explicitly appear in the dimension information. In the case of *Maxpool*, *kernel_size* is reflected in the number of max-related instructions. However, due to compilation optimizations, it is hard to accurately infer the *kernel_size* directly. To precisely recover the attributes of *Maxpool*, NeuroDeX instruments

Algorithm 2: Operator Attribute Recovery

```

Input: List of operators: ops
Output: List of attributes: attrs
attrs  $\leftarrow []$ ;
foreach op  $\in$  ops do
    if “maxpool”  $\in$  op.type then
        in,out  $\leftarrow$  dump_io(op);  $\triangleright$  dump input
        and output tensors of the op
        for k = 1 to in.width do
            stride,padding  $\leftarrow$  infer_sp(k);  $\triangleright$  infer
            stride and padding
            if sim_forward(in,out,k,stride,padding)
            then
                attrs.append([k,stride,padding]);
                 $\triangleright$  simulate forward of the
                op and append when output
                match
            break;
    else if “avgpool”  $\in$  op.type then
        k  $\leftarrow$  extract_attr(op.decompiled);  $\triangleright$  extract
        attributes using LLM
        stride,padding  $\leftarrow$  infer_sp(k);
        attrs.append([k,stride,padding]);
    else if “conv”  $\in$  op.type then
        stride,padding  $\leftarrow$  infer_sp(k);
        attrs.append([k,stride,padding]);
    else if “lrn”  $\in$  op.type or “clip”  $\in$  op.type then
        attr  $\leftarrow$  extract_attr(op.decompiled);
        attrs.append(attr);
    else if “concat”  $\in$  op.type or “transform”
     $\in$  op.type then
        in,out  $\leftarrow$  dump_io(op);
        attr  $\leftarrow$  sim_forward(in,out);
        attrs.append(attr);
return attrs

```

the executable to record the input and output tensors of *Maxpool*. NeuroDeX then enumerates different combinations of *kernel_size*, *stride* and *padding*, simulates the forward of the *Maxpool* until the computed tensor exactly matches the actual output tensor. It is worth noting that any trivial input can achieve full coverage, so NeuroDeX only needs one trivial input to simulate forward. In the case of *Avgpool*, *kernel_size* is evidently reflected in the decompiled code. For example, patterns like “*0.020408(1/49)” repeatedly appear, indicating that *kernel_size* is 7. LLM can extract *kernel_size* from decompiled code to reduce the overhead of dynamic analysis. NeuroDeX infers *stride* and *padding* of *Avgpool* through the constraint enumeration method same with *Conv*.

Local response normalization (lrn) has attributes: *size*, β , α , *bias* and *Clip* has attributes: *min*, *max*. The attributes of lrn and clip generally have a large search space, making them

unsuitable for simulation execution using dynamic analysis enumeration. However, these attributes are often obvious in the decompiled code, which can be extracted directly by LLM. Regarding *Concat*, the sequence of multiple inputs is an attribute that should be extracted. Moreover, at the O3 optimization level in TVM, *Transpose* may be fused after *Concat*. NeuroDeX instruments the executable to record input and output tensors of *Concat*. By enumerating the input order and the number of channel shuffle groups in *Transpose*, NeuroDeX simulates the forward of *Concat* until the computed tensor exactly matches the actual output tensor. Similarly, *Transform* may also involve *Transpose* fused afterward, NeuroDeX determines the attribute values same with *Concat*.

Here is the simplified prompt in operator attribute recovery by LLM:

Simplified prompt of operator attribute recovery

You are an AI assistant specialized in analyzing operators. Given the decompiled code of a {type} operator: {pseudocode}, infer the {attribute}.

D. Model Reconstruction

After recovering operator types and attributes, it is also necessary to restore the computational graph and weights to ultimately construct the high-level model.

To restore the computational graph, NeuroDeX instruments the executable to record the execution sequence of all operator functions and the parameter addresses at each operator’s entry point. All operators have fixed calling conventions, including the number of input and output parameters. By matching the input and output addresses between different functions, We can determine the input-output connection relationships between different operators. The computational graph of the model can be effectively restored finally. For the recovery of model weights, NeuroDeX dumps weights from weight parameter addresses and adjusts the weight layout according to their dimension information. Finally, NeuroDeX converts recovery operators into the corresponding PyTorch model, resulting in a identical reusable high-level model.

During model reconstruction, NeuroDeX needs to adapt to the specific characteristics of quantized compiled models. Quantized compiled methods involves *global_scale* mode and *kl_divergence* mode. Scale refers to the scaling factor between the float domain and int domain during quantized compilation. The *global_scale* method uses the same scale across different operators, and does not rely on data calibration. The *kl_divergence* method needs data for calibration, resulting in higher precision. The weights of quantized compiled models are in the integer domain, and model inference is in integer domain as well. NeuroDeX makes certain adaption to model weights recovery, NeuroDeX also records the parameter types and transforms dumped bytes into corresponding type. Our goal is to recover a reusable, general model with float weights. During model inference, we observe that weights in the integer domain are updated through shift multiplication

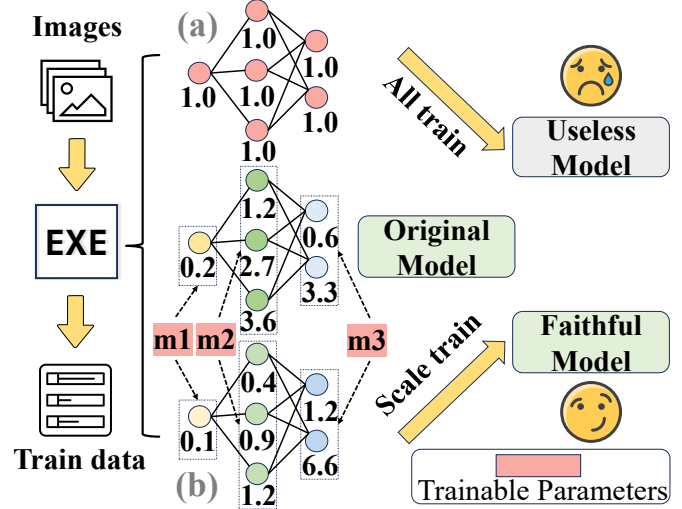


Fig. 3: Analysis of Quantized Compiled Models

(e.g., $weight * (0x6f65c500 >> 0x28)$) to prevent integer overflow. NeuroDeX extracts shifted multiplication value from decompiled code, and compute updated weights: $updated_w = dumped_w \times shifted_multiplication$.

For the *global_scale* method, different operators have same *quant_scale*, so the updated weights are close to the original model’s weights. For the *kl_divergence* method, *quant_scale* adjusts for different operators. Due to compilation optimizations, different *quant_scale* can be confused with regular multiplications, making it difficult to identify them. Eventually, the updated weights are a multiple of the actual weights, and different layers have different multiples. To address this, NeuroDeX adopts a substitute training method illustrated in Figure 3. The target model is the quantized compiled DNN executable, NeuroDeX first prepares query dataset to collect labels in the target executable. Next, NeuroDeX freezes known weights and trains a model that effectively replicates the functionality of the target model.

Typical black-box substitute method for model extraction (a in Figure 3) requires retraining all the model weights, whereas NeuroDeX only needs to train a limited multiples (b in Figure 3). A small amount of training data is enough to gain a model that effectively replicates the functionality of the target model.

IV. EVALUATION SETUP

In the evaluation, we intend to answer the following questions:

- RQ1 (Correctness):** How does NeuroDeX’s performance in correctness compare to State-of-the-Art (SOTA) method?
- RQ2 (Efficiency):** What is the overhead of NeuroDeX compared to SOTA method?
- RQ3 (Comprehensiveness):** Can NeuroDeX cover a wider range of models and different architectures?

TABLE III: Details for the Evaluation Models

Model	Nodes	Edges	Params	Outs
ShuffleNetV2 [29]	229	245	2,294,784	1000
MobileNetV2 [39]	104	115	3,487,816	1000
EfficientNet [50]	188	215	12,966,032	1000
InceptionV1 [47]	143	170	6,998,552	1000
ResNet18 [14]	69	77	11,699,112	1000
VGG16 [44]	41	41	138,357,544	1000
ResNet34 [14]	125	141	21,814,696	1000
SqueezeNet [19]	65	73	1,235,496	1000
MnasNet [49]	151	161	3,200,016	1000
ShuffleNetV1 [60]	203	219	1,420,176	1000
Emotion [1]	46	47	8,757,704	8
SuperRes [43]	10	10	59,657	451,584

RQ4 (Robustness): Can NeuroDeX fix errors encountered during the decompile process and what is the impact of different LLMs on NeuroDeX?

A. Implementation & Environment

We implement NeuroDeX with about 8K LOC Python code and about 1K LOC C++ code. In our experiments, we select GPT-4o [12] for its superior performance in code understanding [58], [61] and the large size (128K) of context window, which is sufficient to cover the operator functions. We conduct experiments on both x86 and aarch64 architectures, we use Intel Pin [28] for dynamic analysis in the x86 architecture, and GDB [7] in the aarch64 architecture. Both Pin and GDB are automated through Pintool scripts and GDB scripts to finish tasks like memory dump. NeuroDeX employs Ghidra [9], a well-known decompiler in reverse engineering, and the version is 11.1.2. NeuroDeX reconstructs DNN executables into high-level models using PyTorch. We statistics and compare the overhead of different methods on AMD EPYC 9654 CPU with 60GB RAM.

B. Baseline & Model Selection

Libsteal and Shi et al.’s work struggle to accurately recover the model, and there is no official code implementation available for these methods. DND and Neuroscope fail to analyze executables with compilation optimizations. DND only analyzes on three small models: MobileNetV2 [39], ResNetV1 [14], and MNIST [4]. The symbolic execution methods in DND introduces significant overhead, limiting its capability to analyze larger models. Neuroscope only supports 12 DNN operators, which limits its usability. What’s more, none of these four decompilers analyze the influence of compiler versions. BTD takes into account compilation optimizations and has been tested on a larger range of models. BTD conducts extensive experiments across different optimization levels and different compiler versions, which demonstrates its effectiveness. Overall, BTD is currently the SOTA method available.

As shown in Table III, to ease of comparison, we evaluate NeuroDeX on six different DL models, comprising a total of 54 DNN executables (varying in compiler, optimization level, and compiler version) that are analyzed in BTD. Moreover,

we have supplemented our evaluation with six more different models, aiming to cover more model structures and varying hyperparameters for same model structure. Furthermore, we conduct an additional analysis on 42 BTD unexplored DNN executables, covering a wider range of compiler versions, architectures, and quantized models. All the executables in our evaluation are stripped.

C. Evaluation Metrics

We evaluate the effectiveness of NeuroDeX from three perspectives: operator type recognition, operator attribute recovery and recovered model inference.

For operator type recognition, we measure Type Recognition Accuracy (TRA). Meanwhile, for operator attribute recovery, we measure Attribute Recovery Accuracy (ARA).

Regarding model inference, we adopt the same method from previous studies [27], [53], which compares the inference results and confidence scores of the recovered model with those of the executables. We regard the inference results as consistent only if the labels and confidence scores are exactly identical or differ solely by negligible precision loss. We employ 100 inputs for the Emotion and SuperRes models and 500 inputs for all other models, calculating Model Inference Accuracy (MIA). For quantized compiled models, the unavoidable precision loss between integer and float domains during quantization and dequantization makes it impossible to recover a model with identical confidence scores. Therefore, we consider the inference correct if the labels match and calculate top-1, top-3, and top-5 of MIA.

V. EVALUATION RESULT

In this section, we show the experimental results to answer the research questions.

A. RQ1: Correctness

To answer RQ1, we compare NeuroDeX with the SOTA method BTD, using the models involved in BTD experiments to demonstrate the performance of NeuroDeX.

BTD uses machine learning to perform operator type recognition and employs symbolic execution methods for operator attribute recovery. BTD can successfully reconstruct nearly identical high-level models from executables compiled by TVM and GLOW in x86 architecture.

However, BTD has some inherent shortcomings. In the operator type recognition stage, BTD trains machine learning model for each compiler version to make predictions. This approach relies heavily on training data and treats the compiler version as prior knowledge, which limits its scalability in real world scenario. Moreover, we find that about 57.9% of the training data in TVM and 18.3% in GLOW appear in the test dataset, further undermining the effectiveness of the method. To avoid the influence of data leak, we randomly split all the data with an 8:2 ratio for train dataset and test dataset, and retrain the model for each compiler version, strictly following the default settings of BTD. As illustrated in Figure 4, we have analyzed BTD’s TRA across different compiler versions.

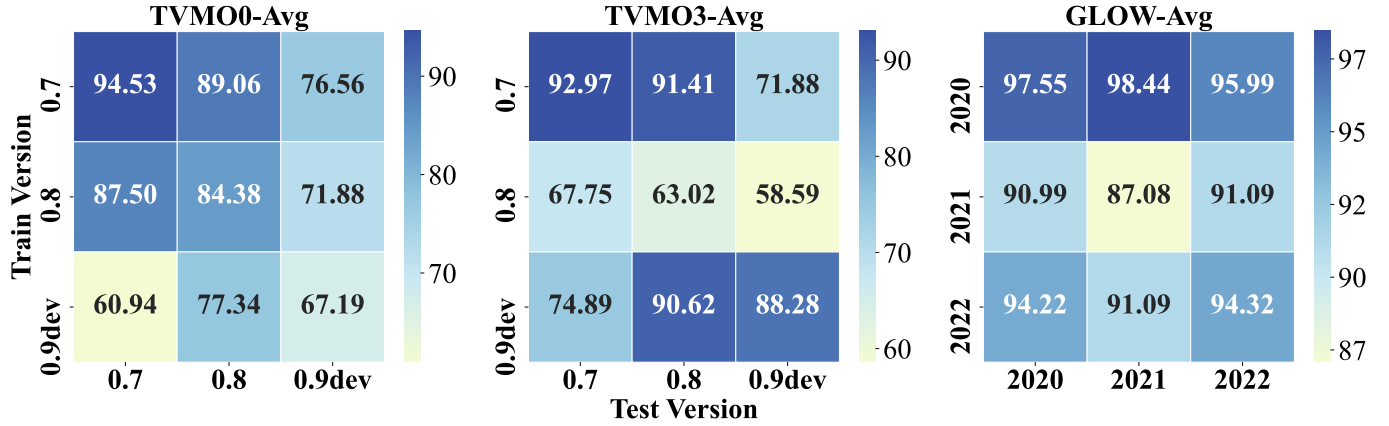


Fig. 4: Retrained BTD Cross Version TRA

TABLE IV: Comparison of TRA between BTD and NeuroDeX (all value in %)

Model	EfficientNet		Inceptionv1		MobileNetv2		ResNet18		ShuffleNetv2		VGG16	
	BTD	NeuroDeX	BTD	NeuroDeX	BTD	NeuroDeX	BTD	NeuroDeX	BTD	NeuroDeX	BTD	NeuroDeX
TVM_v0.7_O0	72.48	97.96	97.1	100	80.47	100	76.56	100	70.05	98.87	84.85	100
TVM_v0.8_O0	39.91	99.28	87.85	100	66.85	100	46.88	100	49.83	98.97	63.64	100
TVM_v0.9dev_O0	40.7	100	86.06	100	64.32	100	34.92	100	39.06	100	53.12	100
TVM_v0.7_O3	35.14	97.3	97.66	98.73	42.86	100	78.79	96.97	77.78	94.44	59.26	88.9
TVM_v0.8_O3	5	90	79.77	92.68	11.76	100	54.55	100	77.14	97.14	70.37	100
TVM_v0.9dev_O3	5.41	100	79.22	100	2.94	100	57.58	100	71.43	100	55.56	100
GLOW_2020	54.24	96.61	77.19	99.04	70.45	95.45	57.14	96.43	86.27	96.08	68.18	86.36
GLOW_2021	58.62	96.55	87.18	98.06	76.74	95.35	54.29	100	94	100	90	95
GLOW_2022	58.62	96.55	87.18	100	76.74	97.67	54.29	100	92	100	90	95

It is evident that BTD’s method exhibits poor cross-version support for compilers after avoiding data leak. Even within the same version, errors of operator type occur to an unacceptable degree, make it difficult to apply directly.

To make the comparison with NeuroDeX more intuitive, we remove the training data that is also on test dataset (operators of the six models in Table IV) and retrain the BTD operator type recognition models following the default settings. The comparison results of TRA are shown in Table IV. The TRA of NeuroDeX significantly outperforms BTD, providing a crucial foundation for accurate operator type recognition, which is essential for subsequent operator attribute recovery and model reconstruction. NeuroDeX achieves results very close to 100% across all experimental models, whereas the BTD method faces relatively severe errors.

As for operator attribute recovery and model reconstruction, NeuroDeX reaches 100% ARA and MIA on all models in TVM; NeuroDeX reaches 100% ARA besides Inceptionv1_2020, ShuffleNetv2_2021, EfficientNet_2020 and EfficientNet_2021 in GLOW. The very few errors in operator attribute recovery are due to occasional wrongs of *Lrn*, *Avgpool* and *Clip*. The attributes of these wrong operators are directly evident in the decompiled code, making it easy to correct them through manual verification. As for MIA in GLOW, one specific situation needs to be addressed: the inference confidence scores of recovered Inceptionv1 by NeuroDeX differ from the executables. When ignoring these confidence

score differences, the class prediction accuracy is 96.4%. The differences in confidence are primarily attributed to precision loss during compilation. Compared to inference results of source high-level ONNX models, the MIA reaches 100%. After correcting all error prediction operators, both ARA and MIA of BTD for all models can achieve 100%. However, it comes at the cost of significant time overhead. We will discuss this issue in detail in RQ2.

Answer to RQ1: NeuroDeX can decompile DNN executables analyzed in BTD under different optimization levels and different compiler versions. NeuroDeX overcomes BTD’s inherent shortcomings in operator type recognition.

B. RQ2: Efficiency

To answer RQ2, we compare the overhead of NeuroDeX with BTD and analyze the underlying reasons.

We choose four models: EfficientNet, ResNet18, Inceptionv1 and ShuffleNetv2. These models cover a range of weights size and topological complexities, enabling a comprehensive evaluation of the overhead associated with BTD and NeuroDeX. The model reconstruction strategies for NeuroDeX and BTD are identical. Therefore, we only compare the time associated with operator type recognition and operator attribute recovery processes. NeuroDeX involves interaction with LLM, which leads to non-fixed time consumption. We measure the time overhead by recording it three times and calculating the

TABLE V: Overhead Analysis on BTD and NeuroDeX (all value in s)

Method	EfficientNet			ResNet18			InceptionV1			ShuffleNetv2		
	TVM_O0	TVM_O3	GLOW	TVM_O0	TVM_O3	GLOW	TVM_O0	TVM_O3	GLOW	TVM_O0	TVM_O3	GLOW
BTD	676.3	265.0	2904.7	468.7	681.2	2416.3	982.8	705.6	4328.8	152.7	92.8	296.2
NeuroDeX	76.9	122.2	204.5	41.4	127.9	129.2	208.3	288.8	304.7	66.0	80.9	75.4

average to ensure a fair comparison. BTD uses IDA [20] to decompile the executables and NeuroDeX uses Ghidra. We overlook the difference from general decompiler preprocessing for fair comparison. The compiler version for our experiment is TVM v0.9dev and GLOW 2022. The overhead of BTD and NeuroDeX is shown in Table V.

For TVM_O0, TVM_O3 and GLOW, the average time spent by BTD is about **6.79** times, **2.77** times, and **12.76** times that of NeuroDeX respectively. The main time overhead for NeuroDeX comes from network request to LLM and dynamic memory monitor. The time of LLM requests can fluctuate due to network conditions. However, in our implementation, requests to LLM are executed through a single thread. Using a multi-threaded approach could easily optimize the time overhead. EfficientNet represents high-capacity and computationally intensive models, while ShuffleNetv2 serves as an example of lightweight model. ResNet18 and InceptionV1 are further included to encompass a broader range of distinct architectural designs. According to our evaluation results, NeuroDeX performs better than BTD in time overhead obviously across all these various models.

Moreover, it is noteworthy that NeuroDeX’s approach does not involve heavy analysis constrained by hardware resources. In contrast, the methods utilized by BTD demand considerable memory and cpu resources, which can lead to performance degradation on consumer-grade devices.

Answer to RQ2: NeuroDeX can decompile DNN executables with a shorter time overhead than SOTA methods and NeuroDeX does not rely heavily on hardware resources.

C. RQ3: Comprehensiveness

To answer RQ3, we aim to evaluate NeuroDeX on a wider range of models and on aarch64 architecture to demonstrate its versatility. We also discuss the compatibility with quantized compiled models of NeuroDeX.

We first evaluate NeuroDeX on the latest compiler version to verify its scalability. According to our observations, TVM is a project that is frequently maintained; GLOW is a stable project, we have counted the commits since 2023, which total only about 100, and the majority are related to feature maintenance and bug fixes. The repository of GLOW has been marked as public archive now. Therefore, we also use NeuroDeX to analyze the latest TVM version (v0.17). We utilize NeuroDeX to decompile RQ1’s six models in TVM 0.17 repeatedly. We evaluate NeuroDeX on six more different models in TVM v0.17, aiming to cover more model structures

TABLE VI: Evaluation of NeuroDeX on the Recent Compiler Version (all value in %)

Model	O0			O3		
	TRA	ARA	MIA	TRA	ARA	MIA
EfficientNet	100	100	100	100	100	100
InceptionV1	100	100	100	97.47	100	100
MobileNetv2	100	100	100	100	100	100
ResNet18	100	100	100	100	100	100
ShuffleNetv2	98.9	100	100	100	100	100
VGG16	100	100	100	100	100	100
MnasNet	99.49	100	100	100	100	100
ResNet34	100	100	100	100	100	100
ShuffleNetv1	100	100	100	97.5	100	100
SqueezeNet	100	97.73	100	100	97.85	100
Emotion	100	100	100	100	100	100
SuperRes	100	100	100	100	100	100

TABLE VII: Evaluation of NeuroDeX on AArch64 Models (all value in %)

Model	O0			O3		
	TRA	ARA	MIA	TRA	ARA	MIA
ShuffleNetv1	100	100	100	100	100	100
ShuffleNetv2	98.9	100	100	100	100	100
MobileNetv2	100	100	100	93.94	100	100
InceptionV1	100	100	100	98.65	100	100
MnasNet	98.97	100	100	100	100	100

and varying hyperparameters for same model structure. The results are shown in Table VI.

NeuroDeX can recover nearly identical high-level models for these 12 models across different optimization levels. In operator type recognition and operator attribute recovery, occasional errors may occur. The former primarily involves errors such as *Avgpool* is incorrectly identified as *Sum*. The latter involves errors in the recognition of *kernel_size* for the *Avgpool*, where the *kernel_size* “*0.00591716 (1/169)” should be 13 but is incorrectly identified as 17. After fixing these errors, the MIA of all models reach 100%.

In order to show the cross-architecture support of NeuroDeX, we also evaluate NeuroDeX on aarch64 in TVM v0.17, the results are shown in Table VII. Based on the experimental results, NeuroDeX can successfully decompile executables across different optimization levels on aarch64 architecture. Some errors may occur in operator type recognition stage. The errors include the incorrect identification of *Avgpool* as *Sum*, as well as misjudgments of activation functions.

As for the evaluation of quantized compiled models, we quantized compile four models including MnasNet, MobileNetv2, ResNet18, ResNet34 using both the *global_scale*

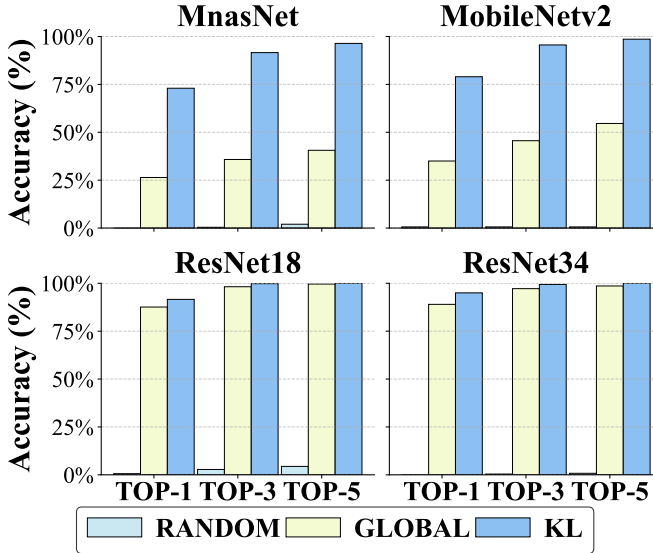


Fig. 5: Evaluation of NeuroDeX on Quantized Compiled Models

and kl_divergence methods in TVM, resulting in eight executables. We decompile these executables using NeuroDeX, the results are shown in Figure 5.

For global_scale method, NeuroDeX can decompile all the four executables with MIA_top1 at least 26.4%, and MIA_top5 at least 40.6%. For kl_divergence method, NeuroDeX can decompile all the four executables with MIA_top1 at least 73.0%, and MIA_top5 at least 96.4%. Given that all models have 1000 output categories, the recovery results are quite satisfactory. In contrast, using the same computational graph with target model and random training with 5000 images (same query dataset with NeuroDeX), the recovered model achieves a maximum MIA_top1 of only 0.6% and a maximum MIA_top5 of only 4.4%, indicating that it almost fails to recover any valuable information. For ResNet18 and ResNet34, NeuroDeX can recover quite similar high-level models under both global_scale and kl_divergence methods. For MnasNet and MobileNetv2, the accuracy of recovered models decreases, we analyze the reasons as follows: compared to ResNet18 and ResNet34, MnasNet and MobileNetv2 have fewer parameters, which makes them more sensitive to the global_scale method. The global_scale method tends to weaken the decision boundaries of models, the queries for recovered model are more likely to be classified into different categories than original high-level models.

Answer to RQ3: We evaluate NeuroDeX on a wider range of models and aarch64 architecture. Results illustrates NeuroDeX's adaptability to various models and different architectures; NeuroDeX can decompile quantized compiled DNN executables and the recovered models are highly similar in functionality to the original models.

D. RQ4: Robustness

To answer RQ4, we classify the error cases encountered by NeuroDeX and introduce specific strategies to fix each type. We also evaluate NeuroDeX on more LLMs.

In operator type recognition, NeuroDeX may occasionally encounter errors. Additionally, due to the inherent output variability of LLMs, repeated analysis might yield different error samples. Nonetheless, our evaluation indicates that the operator type recognition accuracy on all TVM operators reach 99.22%, and it is 97.62% for GLOW, maintaining high accuracy. In operator attribute recovery, the errors are very rare and they are obvious in the decompiled code, such as kernel_size “*0.00591716 (1/169)” should be 13 but is incorrectly identified as 17. Therefore, it does not require a systematic error fix mechanism. We analyze the causes of errors in operator type recognition and the errors can be classified into three categories.

Type 1. A single operator is split into multiple functions.

Type 2. Incorrect recognition of activation functions.

Type 3. Other random operator recognition errors.

The proportions of these three wrong types are 36.2%, 13.8% and 50% respectively. NeuroDeX has corresponding error fix strategies for different types of errors:

Type 1: Error operators exhibit fixed patterns. These errors occur in *Softmax*, *Avgpool* and *Dense_add*. These errors can be detected immediately after operator type recognition. NeuroDeX can fix them by matching predefined patterns of operator partition.

Type 2: These errors can be handled during model reconstruction. By comparing the value of intermediate layer in high-level models with those from instrumented executables, NeuroDeX can locate the different operators and update the activation function according to value difference. After fixing the activation function, NeuroDeX can continuously record the output value of the error operator until it matches the expected value of the executable.

Type 3: These errors can directly lead to crash of model construction. We can observe the exception information of the high-level model to locate error operators. NeuroDeX can locate error operators and fix them by manually checking the decompiled code. After fixing the error operator, NeuroDeX can continuously record the output value of error operator until it matches the expected value of executable.

To demonstrate the effectiveness of NeuroDeX on different LLMs, we also compare the performance of different LLMs including GPT-4.1 [11], Deepseekv3 [24], GPT-4o mini [13], Gemini2.5 flash [8]. The selection of LLMs will affect TRA directly. Results are shown in Table VIII. Deepseekv3 and GPT-4.1 perform well in all models across different compiler settings. Gemini2.5 flash struggles to identify operator of GLOW, GPT-4o mini fails to identify TVM optimization operators and GLOW operators. In summary, NeuroDeX does not rely on a specific LLM. LLMs that perform well in general domains are equally suitable for completing the operator type recognition task.

TABLE VIII: TRA of Different LLMs (all value in %)

LLM	Inceptionv1			ResNet18			MobileNetv2		
	TVM_O0	TVM_O3	GLOW	TVM_O0	TVM_O3	GLOW	TVM_O0	TVM_O3	GLOW
Deepseekv3	100	100	96.12	100	93.94	97.14	100	97.06	100
GPT-4.1	100	100	98.06	100	100	100	100	97.06	97.67
Gemini2.5 flash	99.29	97.47	86.41	100	100	100	98.57	100	81.40
GPT-4o mini	97.87	81.01	36.89	98.31	87.88	31.43	100	94.12	34.88

Answer to RQ4: NeuroDeX has a stable error-fix mechanism that effectively addresses different types of errors. NeuroDeX is not sensitive to the selection of LLMs, and various different LLMs are suitable for NeuroDeX.

VI. DISCUSSION

A. Possible defenses towards NeuroDeX

NeuroDeX targets standard executables compiled using DL compilers and is capable of recovering nearly identical high-level models. Techniques such as binary obfuscation significantly reduce the readability of decompiled code by general-purpose decompilers like Ghidra. This can make NeuroDeX's operator type recognition and operator attribute recovery components ineffective. However, DL compilers do not offer direct support for executable obfuscation, and methods like control flow obfuscation may also negatively impact the speed and accuracy of model inference. Overall, NeuroDeX is designed to handle the most common scenarios effectively. The threat model used in our study is consistent with previous works [27], [42], [53], [54] and is generally common and practical in real-world scenarios.

B. Scalability of NLP models

Related studies [5], [46] indicate that CV models are the majority models on edge devices, and our evaluation focuses on CV models. In contrast, language models have larger search spaces of input and output, as well as greater parameters. Transformer-based models feature complex operator topologies, and operations like attention are decomposed into several low-level operators, further increasing the complexity of the models. This complexity makes it exceedingly difficult to precisely reconstruct an identical model. Currently, NeuroDeX cannot cover this scenario. However, NeuroDeX's core components still provide valuable insights, NeuroDeX can enhance the efficacy of gray-box attacks towards these models. We will address this in future work.

As for LLMs with a large number of parameters, to the best of our knowledge, there is currently no mature solution for compiling them into standalone executables in binary format for inference on edge devices. Existing inference engines of LLMs primarily focus on optimizing the computation process but model weights are typically stored and loaded separately.

C. Downstream Tasks

NeuroDeX can reconstruct high-level model almost identical to the original model, meaning that computational graph,

gradient, weights have been fully exposed, which means that attackers may conduct white-box attacks towards DNN executables on edge devices. Model extraction attacks violate the intellectual property of the model owner. Adversarial examples generated for white-box models can be directly used as inputs for DNN executables, misleading the model's inference results. Moreover, a white-box model allows for weight modification via backdoor injection. Attackers can edit the executables at the addresses where those weights are stored to inject the backdoor. Backdoor injection results in malicious inputs to manipulate the model's behavior, compromising its integrity and reliability. Based on this analysis, NeuroDeX reveals the potential security threats posed to DL compilers. Our discussion of NeuroDeX aims to highlight these security risks to promote the safe use of DL compilers.

VII. RELATED WORK

A. LLM for Reverse Engineering

Recent researches have demonstrated the significant potential of LLMs in reverse engineering, and there are benchmarks available to evaluate their effectiveness [30], [35], [40]. DecGPT [52] leverages LLMs to repair errors in decompiled code, facilitating automatic recompilation. Lmpa [57] and Degpt [16] combine LLMs with program analysis to optimize decompiler's output, restoring more meaningful variable names. ReSym [56] and TypeForge [51] utilize LLMs to recover user-defined structures, enhancing the readability of complex types in decompiled code. LLM4Decompile [48] addresses the limitations of general decompiler and designs an end-to-end decompiler using LLMs. WaDec [41] employs a fine-tuned LLM to interpret and decompile WebAssembly, producing outputs that are more effective than general decompilers. Unlike previous works, NeuroDeX focuses on analyzing DNN executables, utilizing the code understanding capabilities of LLMs to perform tasks such as operator type recognition.

B. On-device Models Security

Many previous works discuss the security of on-device models [32]. Huang et al. design a grey-box adversarial attack framework by comparing deep learning models on Android devices with those from TensorFlow Hub [17], [18]. Sun et al. [46] discover that 41% of machine learning apps do not protect their models at all, and even among those that employ model protection or encryption, 66% can still be extracted. AdvDroid [5] conducts the first systematic study of adversarial attacks on real-world DNN models, revealing that on-device models are also vulnerable to adversarial attacks. Hu

et al. [15] perform an empirical study on on-device models in iOS apps, uncovering security risks associated with deep learning models in the iOS environment. DeMistify [36] can automatically extract on-device models from mobile apps and reuse associated services, successfully executing 82.73% of the models. Many works [27], [53], [59] attempt to decompile on-device models compiled by DL compilers, this is also the threat model of NeuroDeX.

VIII. CONCLUSION

In this work, we design NeuroDeX to provide diverse support in decompiling DNN executables. NeuroDeX recovers DNN executables back into high-level models through operator type recognition, operator attribute recovery and model reconstruction. NeuroDeX leverages the semantic understanding capabilities of LLMs along with dynamic analysis to construct a comprehensive and robust decompilation pipeline. Our evaluations demonstrate that NeuroDeX can successfully decompile DNN executables across different DL compiler settings, different architectures and quantized compiled models.

REFERENCES

- [1] E. Barsoum, C. Zhang, C. C. Ferrer, and Z. Zhang, “Training deep networks for facial expression recognition with crowd-sourced label distribution,” in *Proceedings of the 18th ACM international conference on multimodal interaction*, 2016, pp. 279–283.
- [2] CEVA, “Ceva leverages edge ai to optimize and deploy intelligent systems,” <https://www.ceva-ip.com/wp-content/uploads/2025-Edge-AI-Technology-Report.pdf>, 2025.
- [3] T. Chen, T. Moreau, Z. Jiang, L. Zheng, E. Yan, H. Shen, M. Cowan, L. Wang, Y. Hu, L. Ceze *et al.*, “{TVM}: An automated {End-to-End} optimizing compiler for deep learning,” in *13th USENIX Symposium on Operating Systems Design and Implementation (OSDI 18)*, 2018, pp. 578–594.
- [4] Y. L. Corinna Cortes and C. Burges, “Mnist handwritten digit database,” <http://yann.lecun.com/exdb/mnist/>.
- [5] Z. Deng, K. Chen, G. Meng, X. Zhang, K. Xu, and Y. Cheng, “Understanding real-world threats to deep learning models in android apps,” in *Proceedings of the 2022 ACM SIGSAC Conference on Computer and Communications Security*, 2022, pp. 785–799.
- [6] B. Fang, X. Zeng, and M. Zhang, “Nestdnn: Resource-aware multi-tenant on-device deep learning for continuous mobile vision,” in *Proceedings of the 24th Annual International Conference on Mobile Computing and Networking*, 2018, pp. 115–127.
- [7] GDB, “GDB: The GNU project debugger,” <https://www.gnu.org/software/gdb/>, 2025.
- [8] gemini2.5 flash, <https://deepmind.google/models/gemini/flash/>, 2025.
- [9] Ghidra, “Ghidra software reverse engineering framework,” <https://ghidra-sre.org/>, 2025.
- [10] I. J. Goodfellow, J. Shlens, and C. Szegedy, “Explaining and harnessing adversarial examples,” *arXiv preprint arXiv:1412.6572*, 2014.
- [11] gpt-4.1, <https://openai.com/>, 2025.
- [12] gpt-4o, <https://openai.com/>, 2025.
- [13] gpt-4o mini, <https://openai.com/>, 2025.
- [14] K. He, X. Zhang, S. Ren, and J. Sun, “Deep residual learning for image recognition,” in *Proceedings of the IEEE conference on computer vision and pattern recognition*, 2016, pp. 770–778.
- [15] H. Hu, Y. Huang, Q. Chen, T. Y. Zhuo, and C. Chen, “A first look at on-device models in ios apps,” *ACM Transactions on Software Engineering and Methodology*, vol. 33, no. 1, pp. 1–30, 2023.
- [16] P. Hu, R. Liang, and K. Chen, “Degpt: Optimizing decompiler output with llm,” in *Proceedings 2024 Network and Distributed System Security Symposium*, vol. 267622140, 2024.
- [17] Y. Huang and C. Chen, “Smart app attack: hacking deep learning models in android apps,” *IEEE Transactions on Information Forensics and Security*, vol. 17, pp. 1827–1840, 2022.
- [18] Y. Huang, H. Hu, and C. Chen, “Robustness of on-device models: Adversarial attack to deep learning models on android apps,” in *2021 IEEE/ACM 43rd International Conference on Software Engineering: Software Engineering in Practice (ICSE-SEIP)*. IEEE, 2021, pp. 101–110.
- [19] F. N. Iandola, S. Han, M. W. Moskewicz, K. Ashraf, W. J. Dally, and K. Keutzer, “SqueezeNet: Alexnet-level accuracy with 50x fewer parameters and 0.5 mb model size,” *arXiv preprint arXiv:1602.07360*, 2016.
- [20] IDA, “A powerful disassembler, decompiler and a versatile debugger.” <https://hex-rays.com/>, 2025.
- [21] O. D. Incel and S. Ö. Bursa, “On-device deep learning for mobile and wearable sensing applications: A review,” *IEEE Sensors Journal*, vol. 23, no. 6, pp. 5501–5512, 2023.
- [22] M. Li, Y. Liu, X. Liu, Q. Sun, X. You, H. Yang, Z. Luan, L. Gan, G. Yang, and D. Qian, “The deep learning compiler: A comprehensive survey,” *IEEE Transactions on Parallel and Distributed Systems*, vol. 32, no. 3, pp. 708–727, 2020.
- [23] Y. Li, Y. Jiang, Z. Li, and S.-T. Xia, “Backdoor learning: A survey,” *IEEE transactions on neural networks and learning systems*, vol. 35, no. 1, pp. 5–22, 2022.
- [24] A. Liu, B. Feng, B. Xue, B. Wang, B. Wu, C. Lu, C. Zhao, C. Deng, C. Zhang, C. Ruan *et al.*, “Deepseek-v3 technical report,” *arXiv preprint arXiv:2412.19437*, 2024.
- [25] C. Liu, M. Jobst, L. Guo, X. Shi, J. Partzsch, and C. Mayr, “Deploying machine learning models to ahead-of-time runtime on edge using microtvm,” in *Proceedings of the 2023 Workshop on Compilers, Deployment, and Tooling for Edge AI*, 2023, pp. 37–40.
- [26] H. Liu, Z. Ge, Z. Zhou, F. Shang, Y. Liu, and L. Jiao, “Gradient correction for white-box adversarial attacks,” *IEEE Transactions on Neural Networks and Learning Systems*, 2023.
- [27] Z. Liu, Y. Yuan, S. Wang, X. Xie, and L. Ma, “Decompiling x86 deep neural network executables,” in *32nd USENIX Security Symposium (USENIX Security 23)*, 2023, pp. 7357–7374.
- [28] C.-K. Luk, R. Cohn, R. Muth, H. Patil, A. Klauser, G. Lowney, S. Wallace, V. J. Reddi, and K. Hazelwood, “Pin: building customized program analysis tools with dynamic instrumentation,” *AcM sigplan notices*, vol. 40, no. 6, pp. 190–200, 2005.
- [29] N. Ma, X. Zhang, H.-T. Zheng, and J. Sun, “Shufflenet v2: Practical guidelines for efficient cnn architecture design,” in *Proceedings of the European conference on computer vision (ECCV)*, 2018, pp. 116–131.
- [30] D. Manuel, N. T. Islam, J. Khouri, A. Nunez, E. Bou-Harb, and P. Najaferid, “Enhancing reverse engineering: Investigating and benchmarking large language models for vulnerability analysis in decompiled binaries,” *arXiv preprint arXiv:2411.04981*, 2024.
- [31] S.-M. Moosavi-Dezfooli, A. Fawzi, and P. Frossard, “Deepfool: a simple and accurate method to fool deep neural networks,” in *Proceedings of the IEEE conference on computer vision and pattern recognition*, 2016, pp. 2574–2582.
- [32] T. Nayan, Q. Guo, M. Al Duniawi, M. Botacin, S. Uluagac, and R. Sun, “{SoK}: All you need to know about {On-Device}{ML} model extraction-the gap between research and practice,” in *33rd USENIX Security Symposium (USENIX Security 24)*, 2024, pp. 5233–5250.
- [33] ONNX, “Onnx: Open neural network exchange,” <https://onnx.ai/>, 2025.
- [34] A. Paszke, “Pytorch: An imperative style, high-performance deep learning library,” *arXiv preprint arXiv:1912.01703*, 2019.
- [35] S. Pordanesh and B. Tan, “Exploring the efficacy of large language models (gpt-4) in binary reverse engineering,” *arXiv preprint arXiv:2406.06637*, 2024.
- [36] P. Ren, C. Zuo, X. Liu, W. Diao, Q. Zhao, and S. Guo, “Demistify: Identifying on-device machine learning models stealing and reuse vulnerabilities in mobile apps,” in *Proceedings of the 46th IEEE/ACM International Conference on Software Engineering*, 2024, pp. 1–13.
- [37] N. Rotem, J. Fix, S. Abdulrasool, G. Catron, S. Deng, R. Dzhabarov, N. Gibson, J. Hegeman, M. Lele, R. Levenstein *et al.*, “Glow: Graph lowering compiler techniques for neural networks,” *arXiv preprint arXiv:1805.00907*, 2018.
- [38] A. Salem, R. Wen, M. Backes, S. Ma, and Y. Zhang, “Dynamic backdoor attacks against machine learning models,” in *2022 IEEE 7th European Symposium on Security and Privacy (EuroS&P)*. IEEE, 2022, pp. 703–718.
- [39] M. Sandler, A. Howard, M. Zhu, A. Zhmoginov, and L.-C. Chen, “Mobilenetv2: Inverted residuals and linear bottlenecks,” in *Proceedings*

of the IEEE conference on computer vision and pattern recognition, 2018, pp. 4510–4520.

[40] X. Shang, S. Cheng, G. Chen, Y. Zhang, L. Hu, X. Yu, G. Li, W. Zhang, and N. Yu, “How far have we gone in binary code understanding using large language models,” in *2024 IEEE International Conference on Software Maintenance and Evolution (ICSME)*. IEEE, 2024, pp. 1–12.

[41] X. She, Y. Zhao, and H. Wang, “Wadec: Decompiling webassembly using large language model,” in *Proceedings of the 39th IEEE/ACM International Conference on Automated Software Engineering*, 2024, pp. 481–492.

[42] M. Shi, W. Lin, and W. Deng, “Research on key techniques for reverse engineering of deep learning models for x86 executable files,” in *Proceedings of the 2024 7th International Conference on Computer Information Science and Artificial Intelligence*, 2024, pp. 148–153.

[43] W. Shi, J. Caballero, F. Huszár, J. Totz, A. P. Aitken, R. Bishop, D. Rueckert, and Z. Wang, “Real-time single image and video super-resolution using an efficient sub-pixel convolutional neural network,” in *Proceedings of the IEEE conference on computer vision and pattern recognition*, 2016, pp. 1874–1883.

[44] K. Simonyan and A. Zisserman, “Very deep convolutional networks for large-scale image recognition,” *arXiv preprint arXiv:1409.1556*, 2014.

[45] STMicroelectronics, “Stm32 ai model zoo: Optimized ai models for stm32 microcontrollers,” <https://stm32ai.st.com/model-zoo/>, 2025.

[46] Z. Sun, R. Sun, L. Lu, and A. Mislove, “Mind your weight (s): A large-scale study on insufficient machine learning model protection in mobile apps,” in *30th USENIX security symposium (USENIX security 21)*, 2021, pp. 1955–1972.

[47] C. Szegedy, W. Liu, Y. Jia, P. Sermanet, S. Reed, D. Anguelov, D. Erhan, V. Vanhoucke, and A. Rabinovich, “Going deeper with convolutions,” in *Proceedings of the IEEE conference on computer vision and pattern recognition*, 2015, pp. 1–9.

[48] H. Tan, Q. Luo, J. Li, and Y. Zhang, “Llm4decompile: Decompiling binary code with large language models,” *arXiv preprint arXiv:2403.05286*, 2024.

[49] M. Tan, B. Chen, R. Pang, V. Vasudevan, M. Sandler, A. Howard, and Q. V. Le, “Mnasnet: Platform-aware neural architecture search for mobile,” in *Proceedings of the IEEE/CVF conference on computer vision and pattern recognition*, 2019, pp. 2820–2828.

[50] M. Tan and Q. Le, “Efficientnet: Rethinking model scaling for convolutional neural networks,” in *International conference on machine learning*. PMLR, 2019, pp. 6105–6114.

[51] Y. Wang, R. Liang, Y. Li, P. Hu, K. Chen, and B. Zhang, “Typeforge: Synthesizing and selecting best-fit composite data types for stripped binaries,” in *2025 IEEE Symposium on Security and Privacy (SP)*. IEEE Computer Society, 2025, pp. 2847–2864.

[52] W. K. Wong, H. Wang, Z. Li, Z. Liu, S. Wang, Q. Tang, S. Nie, and S. Wu, “Refining decompiled c code with large language models,” *arXiv preprint arXiv:2310.06530*, 2023.

[53] R. Wu, T. Kim, D. J. Tian, A. Bianchi, and D. Xu, “{DnD}: A {Cross-Architecture} deep neural network decompiler,” in *31st USENIX Security Symposium (USENIX Security 22)*, 2022, pp. 2135–2152.

[54] R. Wu, M. Zou, A. Khan, T. Kim, D. Xu, D. J. Tian, and A. Bianchi, “Neuroscope: Reverse engineering deep neural network on edge devices using dynamic analysis,” in *34th USENIX Security Symposium (USENIX Security 25)*, 2025.

[55] X. Wu, J. Yang, L. Ma, Y. Xue, and J. Zhao, “On the usage and development of deep learning compilers: an empirical study on tvm,” *Empirical Software Engineering*, vol. 27, no. 7, p. 172, 2022.

[56] D. Xie, Z. Zhang, N. Jiang, X. Xu, L. Tan, and X. Zhang, “Resym: Harnessing llms to recover variable and data structure symbols from stripped binaries,” in *Proceedings of the 2024 on ACM SIGSAC Conference on Computer and Communications Security*, 2024, pp. 4554–4568.

[57] X. Xu, Z. Zhang, S. Feng, Y. Ye, Z. Su, N. Jiang, S. Cheng, L. Tan, and X. Zhang, “Lmpa: Improving decompilation by synergy of large language model and program analysis,” *arXiv preprint arXiv:2306.02546*, 2023.

[58] Z. Yu, Y. Zhao, A. Cohan, and X.-P. Zhang, “Humaneval pro and mbpp pro: Evaluating large language models on self-invoking code generation,” *arXiv preprint arXiv:2412.21199*, 2024.

[59] J. Zhang, P. Wang, and D. Wu, “Libsteal: Model extraction attack towards deep learning compilers by reversing dnn binary library,” in *Proceedings of the 18th International Conference on Evaluation of Novel Approaches to Software Engineering (ENASE)*, 2023.

[60] X. Zhang, X. Zhou, M. Lin, and J. Sun, “Shufflenet: An extremely efficient convolutional neural network for mobile devices,” in *Proceedings of the IEEE conference on computer vision and pattern recognition*, 2018, pp. 6848–6856.

[61] Y. Zhao, Z. Luo, Y. Tian, H. Lin, W. Yan, A. Li, and J. Ma, “Codejudge-eval: Can large language models be good judges in code understanding?” *arXiv preprint arXiv:2408.10718*, 2024.

IX. APPENDIX

A. Support Operator List

TVM:

concat, split, pad, flatten, transform, reshape, expand_dim, transpose, add, sub, mul, div, power, softmax, sqrt, rsqrt, flatten, clip, neg, abs, lrn, relu, exp, maxpool, avgpool, sum, max, conv2d, dense.

TVM_fused:

conv2d · (mul|add)* · (activation)?, dense · (mul|add)* · (activation)?, add · (activation)?, concat · (reshape · transpose · reshape)? · (activation)?, concat · (reshape · transpose · reshape)? · split, reshape · transpose · reshape.

GLOW:

maxpool, avgpool, softmax, relu, lrn, add, sub, mul, dense, conv2d, convdkkc8, conv2d_relu, conv2d_clip, tensor_transformation (insert_tensor, extract_tensor...).

B. Supplementary examples of GLOW

Figure 6 is the example of *Conv* and *Pooling* in GLOW. *Kernel_size* of GLOW and output channel of *Pooling* can be extracted for the decompiled code.

C. More Evaluation of BTD

As a multi-classification machine learning model, BTD can also be evaluated based Type Hamming Accuracy(THA):

$$THA = \frac{1}{N} \sum_{i=1}^N (Pred_i == Label_i) \quad (4)$$

where N denotes the number of operator classes, and it’s also the length of the prediction vector for a single sample. The average result of TRA and THA for different compiler versions are shown in Table IX. Although THA may achieve higher results, TRA undoubtedly provides a more scientific measure of the true effectiveness of operator recognition. For instance, prediction-label pair like $[1, 0, 0, 0, 0 \dots]_{20}$ and $[0, 1, 0, 0, 0 \dots]_{20}$ will yield THA with $18/20 = 0.9$, but from the operator functional perspective, it is entirely incorrect.

D. Conv vs ConvDKKC8

In GLOW, there are two specific types of *Conv2d*: the standard *Conv2d* and the optimized *Conv2d*, known as *ConvDKKC8*, which kernel parameter dimension is optimized into $[O_c/8, I_c, K, K, 8]$. NeuroDeX records memory read during operator execution and tracks the address offset of output channels throughout the execution process.

For the standard *Conv2d*, it satisfies:

$$\frac{\text{offset}}{\text{in_channel} \times \text{kernel_size}^2} == 1 \quad (5)$$

```

void FUN_00402b40(long param_1, long
param_2,
long param_3, undefined4 *param_4)
{
do{
    ...
    }while (lVar16 != 0x5400);
    ...
    }while (lVar12 != 0x38);
    ...
    }while (uVar18 != 3);
    ...
    }while (uVar9 != 3);
    if(lVar14 == 0x60){
        return;
    }
}while(true);
}
    kernel size of conv is: 3

```



```

void FUN_00402380(long param_1, undefined4
*param_2)
{
do{
    ...
    }while (lVar6 != 0);
    ...
    }while (uVar21 < uVar11);
    ...
    }while (lVar5 != 0x18);
    ...
    }while (lVar16 != 0x38);
    ...
    }while (lVar8 != 0x38);
    ...
    return;
}
    output channel of maxpool is: 24

```

Fig. 6: Glow Example of Conv and Pooling

TABLE IX: TRA and THA of BTD (consistent with Table IV) on Different Compiler Versions (all value in %)

Metric	TVM_O0			TVM_O3			GLOW		
	v0.7	v0.8	v0.9dev	v0.7	v0.8	v0.9dev	2020	2021	2022
TRA_Avg	80.4	64.43	61.31	70.33	57.67	54.86	72.57	79.36	78.99
THA_Avg	96.42	94.57	98.50	98.04	97.05	97.10	97.33	98.48	96.91

For the *ConvDKKC8*, it satisfies:

$$\frac{\text{offset}}{\text{in_channel} \times \text{kernel_size}^2} == 8 \quad (6)$$